

# Solution-processed anthradithiophene–PCBM p–n junction photovoltaic cells fabricated by using the photoprecursor method

Hiroko Yamada<sup>a,d</sup>, Yuji Yamaguchi<sup>b</sup>, Ryuta Katoh<sup>c</sup>, Takao Motoyama<sup>b</sup>, Tatsuya Aotake<sup>a</sup>, Daiki Kuzuhara<sup>a</sup>, Mitsuharu Suzuki<sup>a</sup>, Tetsuo Okujima<sup>c</sup>, Hidemitsu Uno<sup>c</sup>, Naoki Aratani<sup>a</sup>, and Ken-ichi Nakayama<sup>a,b,d</sup>

Received (in XXX, XXX) Xth XXXXXXXXXX 200X, Accepted Xth XXXXXXXXXX 200X

First published on the web Xth XXXXXXXXXX 200X

DOI: 10.1039/b000000x

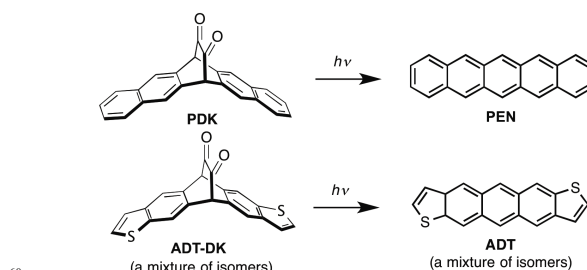
**P–n junction solar cells based on anthradithiophene (ADT) as p-type semiconductor were fabricated by using the photoprecursor method in which an  $\alpha$ -diketone-type precursor was spin-coated and then transformed to ADT in situ by photoirradiation. Combination with PC<sub>71</sub>BM as n-layer material led to 1.54% photoconversion efficiency.**

Solution-processable organic semiconductors are expected to enable the fabrication of low-cost, large-area electronic devices by simple deposition techniques.<sup>1</sup> Along this line, a variety of soluble low band gap polymers<sup>2</sup> and molecular materials<sup>3</sup> have been developed in order for achieving cost-effective, high-performance organic solar cells. High photoconversion efficiencies (PCEs) of over 8% have already been realized with these materials in bulk-heterojunction-type devices.<sup>2,3</sup>

Besides bulk heterojunction cells, it has been shown that organic solar cells in a multilayer structure, especially the p–i–n structure, can also afford high PCEs.<sup>4</sup> An advantage associated with the multilayer configuration is that one can have more precise control over the morphology and material distribution within the active layer, which would contribute to, for example, improving the electrode–organic interface properties and decreasing leak current. However, solution deposition processes are typically not suitable for making layer-by-layer structures, and more costly vacuum deposition is commonly employed. The precursor method has recently been the focus of attention in order to resolve this issue and achieve layer-by-layer structures by solution deposition. In this context, thermally convertible precursors have been developed to employ intact acenes,<sup>5,6</sup> phthalocyanines,<sup>7</sup> benzoporphyrins,<sup>8</sup> oligothiophenes,<sup>9</sup> diketopyrrolopyrroles,<sup>10</sup> quinacridones<sup>11</sup> and indigos<sup>12</sup> in solution-processed devices to take advantage of their favourable photoelectronic properties.<sup>13</sup> This approach has also been applied to polymer-based devices.<sup>14</sup>

Several groups including us reported photoconvertible precursors of acenes which can be converted to the corresponding acenes in solution or thin films quantitatively.<sup>6,15,16</sup> In addition, it has been demonstrated that acene-based thin films prepared by the photoprecursor approach can be used in electronic devices; e.g., a hole mobility of 0.86 cm<sup>2</sup> V<sup>-1</sup> s<sup>-1</sup> was obtained in a top-contact-type thin-film transistor (TFT) based on pentacene (PEN) photogenerated in situ from the corresponding  $\alpha$ -diketone-type precursor (PDK, Scheme 1).<sup>17</sup> Here, the photoconversion of  $\alpha$ -diketone derivatives can proceed at room temperature or lower, though higher device performance sometimes results when gentle heating (<100 °C) is applied during the reaction.

This unnecessary of intense heating is highly beneficial in that organic devices can be fabricated on thermolabile substrates.

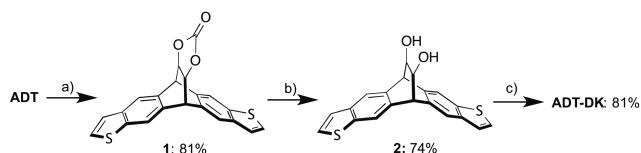


**Scheme 1** Photoreaction of the precursors to acenes.

Recent progress in search for new organic semiconductors has shown that thiophene-based molecular compounds, especially fused-thiophene aromatics, often afford superior device performances owing to their favourable intermolecular interactions in nanocrystalline films, such as van der Waals interactions,  $\pi$ – $\pi$  stacking, and sulfur–sulfur contacts.<sup>18</sup> One of the representative compounds in this class is anthradithiophene (ADT, Scheme 1), which possesses a similar electric structure to that of PEN.<sup>19</sup> In this communication, we will report the synthesis, characterization, and photoreaction of ADT-DK, the  $\alpha$ -diketone-type photoprecursor of ADT. In addition, p–n junction organic photovoltaic (OPV) devices based on ADT as p-layer material were fabricated by the photoprecursor method by using ADT-DK as precursor. [6,6]-Phenyl-C<sub>61</sub>- or C<sub>71</sub>-butyric acid methyl ester (PC<sub>61</sub>BM or PC<sub>71</sub>BM) was employed as n-layer material, and the performance of the resulting devices was evaluated in comparison with PEN–PCBM devices. The obtained results show high potential of ADT as a p-layer material to be used in OPV devices fabricated by using the photoprecursor approach.

The parent ADT was prepared as a syn–anti isomeric mixture following the previously reported procedure.<sup>19a</sup> The precursor ADT-DK was prepared from the parent ADT in three steps as shown in Scheme 2: (1) Diels–Alder reaction of ADT with vinylene carbonate at 180 °C for 3 days to give **1** in 81% yield; (2) deprotection in basic conditions to give diol **2** in 74% yield; (3) Swern oxidation of **2** to give ADT-DK in 81% yield. The compounds were characterized by <sup>1</sup>H and <sup>13</sup>C NMR and mass spectrometry. The structure of ADT-DK was also confirmed by single-crystal X-ray analysis (ESI<sup>†</sup>, Figure S1).<sup>‡</sup> The syn–anti isomers of ADT-DK are randomly distributed at 50:50 ratio in crystals.

The UV–vis absorption spectra of ADT and ADT-DK are shown in ESI<sup>†</sup>, Figure S2. ADT-DK shows a broad absorption around 460 nm, which can be attributed to the n– $\pi^*$



**Scheme 2** Synthesis of **ADT-DK**. Reagents and conditions: a) vinylene carbonate, xylenes, autoclave, 180 °C, 3 days; b) 4M NaOH, THF, reflux, 2 h; c) TFAA, DMSO, DIPEA, *dry*-CH<sub>2</sub>Cl<sub>2</sub>, -60 °C, 1.5 h.

absorption of the diketone moiety. The photoreaction of **ADT-DK** to **ADT** was monitored by the change in UV-vis absorption (ESI<sup>†</sup>, Figure S2). A toluene solution of **ADT-DK** (0.2 mg in 10 ml) was bubbled with argon, and the solution was irradiated by a 500 W xenon lamp through a monochromator ( $\lambda_{\text{EX}} = 468 \text{ nm}$ ,  $14.9 \text{ mW cm}^{-2}$ ). The reaction finished in 17.5 min in this case. The photoreaction of **ADT-DK** was also performed in a spin-coated thin film, and the complete conversion to **ADT** was confirmed by IR spectra (ESI<sup>†</sup>, Figure S3); namely, the C=O stretching band at  $1730 \text{ cm}^{-1}$  disappeared after irradiation by a blue LED lamp for 30 min in a glove box. The ionization potential of thus obtained **ADT** film was determined to be 5.1 eV by photoelectron spectroscopy (ESI<sup>†</sup>, Figure S4). This value is comparable with that obtained for a thin film of directly deposited anthra(2,3-*b*:6,7-*b'*)dithiophene (*anti*-**ADT**).<sup>19b</sup>

Solution-processed p-n junction devices based on photogenerated acene and PC<sub>61</sub>BM were typically fabricated as follows (Figure 1): After spin-coating of PEDOT:PSS on ITO, **PDK** or **ADT-DK** in CHCl<sub>3</sub> (5 mg ml<sup>-1</sup>) was spin-coated at 800 rpm for 30 sec then irradiated by a blue LED at rt for 30 min. On top of that, PC<sub>61</sub>BM in CHCl<sub>3</sub> (10 mg ml<sup>-1</sup>) was spin-coated at 800 rpm for 30 sec, then Ca (10 nm) and Al (80 nm) were sequentially deposited. This process affords devices with a structure described as [ITO / PEDOT:PSS (30 nm) / Acene (40 nm) / PC<sub>61</sub>BM (40 nm) / Ca (10 nm) / Al (80 nm)].

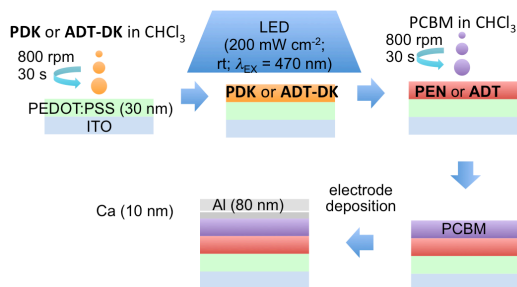


**Figure 1** Schematic diagram of fabrication of p-n junction OPV devices.

The photovoltaic performance of the obtained devices is summarized in Figure 2 and Table 1. The device based on **PEN** and PC<sub>61</sub>BM showed a PCE of 0.25% (short circuit current density,  $J_{\text{SC}} = 0.80 \text{ mA cm}^{-2}$ ; open circuit voltage,  $V_{\text{OC}} = 0.52 \text{ V}$ ; fill factor,  $FF = 0.59$ ). By replacing **PEN** with **ADT**, PCE increased by approximately three times to 0.74% ( $J_{\text{SC}} = 1.91 \text{ mA cm}^{-2}$ ,  $V_{\text{OC}} = 0.61 \text{ V}$  and  $FF = 0.64$ ). Employment of PC<sub>71</sub>BM instead of PC<sub>61</sub>BM led to a considerably higher  $J_{\text{SC}}$  value,<sup>18</sup> resulting in an even higher PCE of 1.54% ( $J_{\text{SC}} = 3.46 \text{ mA cm}^{-2}$ ,  $V_{\text{OC}} = 0.67 \text{ V}$ ;  $FF = 0.66$ ). In this case again, the **ADT**-based device showed a PCE approximately three times higher than that of the **PEN**-based counterpart (PCE = 0.44,  $J_{\text{SC}} = 1.56 \text{ mA cm}^{-2}$ ,  $V_{\text{OC}} = 0.53 \text{ V}$ ;  $FF = 0.53$ ).

To evaluate the influence of n-layer thickness, a few **ADT-PC**<sub>71</sub>BM devices were additionally prepared using PC<sub>71</sub>BM solutions of different concentrations from 5 to 20 mg ml<sup>-1</sup>,

which corresponds to the resulting film thickness of 13–116 nm. (The film thicknesses were summarized in Table S1 in ESI<sup>†</sup>) The best performance was achieved at 10 mg ml<sup>-1</sup> concentration (40 nm film thickness). When the PC<sub>71</sub>BM film is thicker,  $J_{\text{SC}}$  decreased because of the higher resistance of the film. With a thinner PC<sub>71</sub>BM film,  $V_{\text{OC}}$  decreased because of the higher leak current.

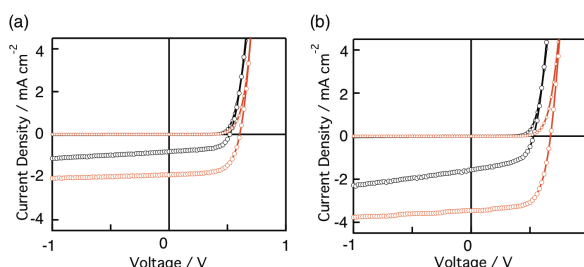


**Figure 2** (a)  $I$ - $V$  curves for **PEN-PC**<sub>61</sub>BM (black lines) and **ADT-PC**<sub>61</sub>BM (red lines) devices; (b)  $I$ - $V$  curves of **PEN-PC**<sub>71</sub>BM (10 mg ml<sup>-1</sup>) (black lines) and **ADT-PC**<sub>71</sub>BM (red lines) devices; larger circles: under AM 1.5G illumination; smaller circles: in the dark.

**Table 1** Performance of the acene-PCBM p-n junction OPV devices.

acene	PCBM(mg ml <sup>-1</sup> ) <sub>i</sub>	$J_{\text{SC}} / \text{mA cm}^{-2}$	$V_{\text{OC}} / \text{V}$	$FF$	PCE / %	$R_s / \text{ohm cm}^{-2}$	$R_p / \text{ohm cm}^{-2}$
<b>PEN</b>	PC <sub>61</sub> BM(10)	0.80	0.52	0.59	0.25	57	2416
<b>ADT</b>	PC <sub>61</sub> BM(10)	1.91	0.61	0.64	0.74	31	5052
<b>PEN</b>	PC <sub>71</sub> BM(10)	1.56	0.53	0.53	0.44	45	1015
<b>ADT</b>	PC <sub>71</sub> BM(5)	2.08	0.49	0.53	0.53	42	888
<b>ADT</b>	PC <sub>71</sub> BM(10)	3.46	0.67	0.66	1.54	24	13336
<b>ADT</b>	PC <sub>71</sub> BM(15)	2.49	0.66	0.58	0.95	69	2522
<b>ADT</b>	PC <sub>71</sub> BM(20)	1.82	0.64	0.48	0.56	194	3116

The incident photon-to-current conversion efficiency (IPCE) curves and the UV-vis spectra of the acene-PCBM (10 mg ml<sup>-1</sup>) devices are shown in Figure 3. By using PC<sub>71</sub>BM, the absorbance of the multilayer films in visible region increased by 1.5 to 2 times compared to the cases when PC<sub>61</sub>BM was used.<sup>20a</sup> Furthermore, the **ADT** device showed higher performance than the **PEN** device in each case, although the absorption abilities are comparable to each other.

The slightly higher  $V_{\text{OC}}$  of the **ADT** device is attributed to the deeper HOMO level of **ADT** (5.1 eV) compared to **PEN** (5.0 eV). The photocurrent in reverse voltage (Figure 2) was nearly constant in the **ADT** device, whereas it increases in the **PEN** device with increasing reverse voltage, which is reflected in the higher  $FF$ , lower series resistance ( $R_s$ ), and higher parallel resistance ( $R_p$ ) in the **ADT** device. This difference indicates that the p-layer based on **ADT** has higher charge extraction ability; i.e., higher charge mobility. To check the film structures of **PEN** and **ADT** prepared by photoconversion, X-ray diffraction pattern of the films were measured (ESI<sup>†</sup>, Figure S5). For the **PEN** film, a peak corresponding to a  $d$ -space of 15.1 Å was observed, suggesting the edge-on arrangement of **PEN** molecules.<sup>21</sup> On the other hand, the **ADT** film gave a featureless trace without any recognizable peaks. This implies that the randomly oriented **ADT** film is more suitable for charge extraction in the device, compared to the **PEN**-based film with the edge-on arrangement having less overlap of  $\pi$ -orbitals along the vertical direction.<sup>22</sup>

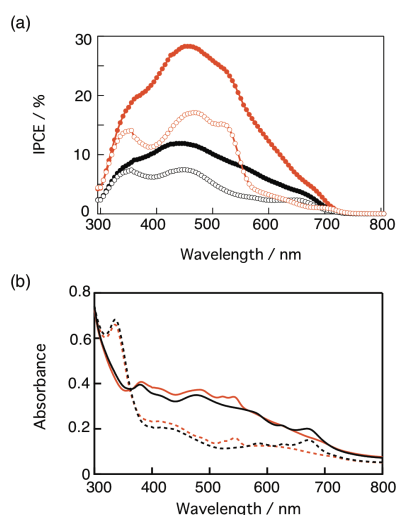


**Figure 3** (a) IPCE curves of [ITO / PEDOT:PSS / acene / PCBM / Ca / Al] and (b) absorption spectra of the same active layer films on ITO / PEDOT:PSS without the Ca and Al layers: **PEN** / PC<sub>61</sub>BM (black open circles for (a); black broken line for (b)); **ADT** / PC<sub>61</sub>BM (red open circles for (a); black red line for (b)); **PEN** / PC<sub>71</sub>BM (black closed circles for (a); black solid line for (b)); **ADT** / PC<sub>71</sub>BM (red closed circles for (a); red solid line for (b)). The concentration of PCBM solutions is 10 mg ml<sup>-1</sup>.

Bulk heterojunction devices with acenes as p-type and PC<sub>61</sub>BM as n-type materials were also evaluated; however, the PCE values were less than 0.1% with significantly low *J*<sub>sc</sub> values. Considering the high crystallinity of **PEN** and **ADT**, the well-mixed i-layers might not be formed in combination with PC<sub>61</sub>BM.

In summary, we were successful to prepare p-n heterojunction solar cells based on **ADT** and PCBM via the photoprecursor method for the first time. The PCE of the best performed **ADT**-PC<sub>71</sub>BM device is 1.54%, which is a significant improvement from the 0.25% PCE obtained with our prototype **PEN**-PC<sub>61</sub>BM device prepared by the same method. The results clearly demonstrate that the photoprecursor method makes hardly soluble organic semiconductors such as **ADT** well compatible with solution-based deposition techniques. In addition, the photoprecursor approach enables the formation of multilayer structures by solution processes. These achievements pave the way to a widely applicable methodology for the construction of sophisticated multilayer structures (e.g., p-i-n type triple-layer structures) by solution processes. Further research along these lines is underway.

## Notes and references

<sup>a</sup> Graduate School of Materials Science, Nara Institute of Science and Technology, 8916-5, Ikoma, Nara 630-0192, Japan. Fax: +81-743-72-6042; Tel: +81-743-72-6041; E-mail: hyamada@ms.naist.jp

<sup>b</sup> Department of Electrical Devices, Graduate School of Science and Engineering, Yamagata University, Yonezawa 992-8510, (Japan), Fax: (+81)238-26-3713, E-mail: nakayama@yz.yamagata-u.ac.jp

<sup>c</sup> Graduate School of Science and Engineering, Ehime University, Matsuyama 790-8577, Japan

<sup>d</sup> CREST, JST, Chiyoda-Ku, Tokyo 102-0075, Japan

† Electronic Supplementary Information (ESI) available: [details of any supplementary information available should be included here]. See DOI: 10.1039/b000000x/

‡ Crystallographic data for **ADT-DK**: C<sub>20</sub>H<sub>10</sub>O<sub>2</sub>S<sub>2</sub>, M = 346.42, orthorhombic, space group *Fdd*<sub>2</sub> (#43), *a* = 27.54611, *b* = 33.092(13), *c* = 6.766(3) Å, *V* = 6156(4) Å<sup>3</sup>, *T* = 100 K, *Z* = 16, *R*<sub>1</sub> = 0.0448, *wR*<sub>2</sub> =

0.1028, GOF = 1.086. CCDC 955408 contains the supplementary crystallographic data.

- a) M. Mas-Torrent and C. Rovira, *Chem. Soc. Rev.*, 2008, **37**, 827. b) J. E. Anthony, *Angew. Chem. Int. Ed.*, 2008, **47**, 452. c) A. R. Murphy and J. M. J. Fréchet, *Chem. Rev.*, 2007, **107**, 1096.
- a) C. Duan, F. Huang, and Y. Cao, *J. Mater. Chem.*, 2012, **22**, 10416. b) H. Zhou and W. You, *Macromolecules*, 2012, **45**, 607. c) P.-L. T. Boudreault, A. Najari and M. Leclerc, *Chem. Mater.*, 2011, **23**, 456. d) C. L. Chochos and S. A. Choulis, *Prog. Polym. Sci.*, 2011, **36**, 1326. e) Y.-J. Cheng, S.-H. Yang and C.-S. Hsu, *Chem. Rev.*, 2009, **109**, 5868. f) J. Chen and Y. Cao, *Acc. Chem. Res.*, 2009, **42**, 1709. g) Y. Liang and L. Yu, *Acc. Chem. Res.*, 2009, **42**, 1227.
- a) A. Mishra and P. Bauerle, *Angew. Chem. Int. Ed.*, 2012, **51**, 2020. b) Y. Lin, Y. Li and X. Zhan., *Chem. Soc. Rev.*, 2012, **41**, 4245. c) B. Walker, C. Kim, and T.-C. Nguyen., *Chem. Mater.*, 2011, **23**, 470. d) F. Würthner and K. Meerholz, *Chem. Eur. J.*, 2010, **16**, 9366.
- a) D. Gebeyehu, M. Pfeiffer, B. Maennig, J. Drechsel, A. Werner and K. Leo, *Thin Solid Films*, 2004, **451/452**, 29. b) K. Suemori, T. Miyata, M. Yokoyama and M. Hiramoto, *Appl. Phys. Lett.*, 2005, **86**, 063509. c) Y. Matsuo, Y. Sato, T. Niinomi, I. Soga, H. Tanaka and E. Nakamura, *J. Am. Chem. Soc.*, 2009, **131**, 16048.
- a) P. T. Herwig and K. Müllen, *Adv. Mater.*, 1999, **11**, 480. b) A. Afzali, C. D. Dimitrakopoulos and T. L. Breen, *J. Am. Chem. Soc.*, 2002, **124**, 8812. c) J. Xiao, H. M. Duong, Y. Liu, W. Shi, L. Ji, G. Li, S. Li, X.-W. Liu, J. Ma, F. Wudl and Q. Zhang, *Angew. Chem. Int. Ed.*, 2012, **51**, 6094.
- M. Watanabe, K.-Y. Chen, Y. J. Chang and T. J. Chow, *Acc. Chem. Res.*, 2013, **46**, 1606. And references cited therein.
- a) T. Akiyama, A. Hirao, T. Okujima, H. Yamada, H. Uno and N. Ono, *Heterocycles*, 2007, **74**, 835. b) A. Hirao, T. Akiyama, T. Okujima, H. Yamada, H. Uno, Y. Sakai, S. Aramaki and N. Ono, *Chem. Commun.*, 2008, 4714.
- S. Ito, T. Murashima, H. Uno and N. Ono, *Chem. Commun.*, 1998, 1661.
- A. R. Murphy, J. M. J. Fréchet, P. Chang, J. Lee and V. Subramanian, *J. Am. Chem. Soc.*, 2004, **126**, 1596.
- J. S. Zambounis, Z. Hao, A. Iqbal, *Nature*, 1997, **388**, 131.
- T. L. Chen, J. J.-A. Chen, L. Catane and B. Ma, *Org. Electron.*, 2011, **12**, 1126.
- E. D. Glowacki, G. Voss, K. Demirak, M. Havlicek, N. Sünger, A. C. Okur, U. Monkowius, J. Ga siorowski, L. Leonat and N. S. Sariciftci, *Chem. Commun.*, 2013, **49**, 6063.
- H. Yamada, T. Okujima and N. Ono, *Chem. Commun.*, 2008, 2957.
- H. Yamada, Y. Yamashita, M. Kikuchi, H. Watanabe, T. Okujima, H. Uno, T. Ogawa, K. Ohara and N. Ono, *Chem. Eur. J.*, 2005, **11**, 6212.
- a) J. H. Edwards and W. J. Feast, *Polymer*, 1980, **21**, 595. b) L. H. Nguyen, S. Günes, H. Neugebauer, N. S. Sariciftci, F. Banishoeb, A. Henckens, T. Cleij, L. Lutsen and D. Vanderzande, *Sol. Energy Mater. Sol. Cells*, 2006, **90**, 2815.
- a) J. Strating, B. Zwanenburg, A. Wagenaar and A. C. Udding, *Tetrahedron Lett.*, 1969, **10**, 125. b) R. Mondal, B. K. Shah and D. C. Neckers, *J. Am. Chem. Soc.*, 2006, **128**, 9612. c) C. Tönshoff and H. F. Bettinger, *Angew. Chem. Int. Ed.*, 2010, **49**, 4125. d) references cited in ref 13.
- K. Nakayama, C. Ohashi, Y. Oikawa, T. Motoyama and H. Yamada, *J. Mater. Chem. C.*, 2013, **1**, 6244.
- K. Takimiya, S. Shinamura, I. Osaka and E. Miyazaki, *Adv. Mater.*, 2011, **23**, 4347.
- a) J. G. Laquindanum, H. E. Katz and A. J. Lovinger, *J. Am. Chem. Soc.*, 1998, **120**, 664. b) M. Nakano, K. Niimi, E. Miyazaki, I. Osaka, K. Takimiya, *J. Org. Chem.*, 2012, **77**, 8099.
- a) M. M. Wienk, J. M. Kroon, W. J. H. Verhees, J. Knol, J. C. Hummelen, P. A. van Hal and R. A. J. Janssen, *Angew. Chem. Int. Ed.*, 2003, **42**, 3371. b) Karl Leo, *Appl. Phys. Lett.*, 2009, **94**, 223307.
- C. D. Dimitrakopoulos and P. R. L. Malenfant, *Adv. Mater.*, 2002, **14**, 99.
- Preliminary space charge limited current measurements gave hole mobilities along the vertical direction of  $3.41 \times 10^{-4}$  and  $1.06 \times 10^{-4}$  cm<sup>2</sup> V<sup>-1</sup> s<sup>-1</sup> in **ADT** and **PEN**, respectively. See ESI<sup>†</sup>, Figure S6.